SPECIAL ISSUE ON STRUCTURE IN GLASSY AND JAMMED SYSTEMS

Tuning pairwise potential can control the fragility of glass-forming liquids: from a tetrahedral network to isotropic soft sphere models

Journal of Statistical Mechanics: Theory and Experiment
An IOP and SISSA journal

Special Issue on Structure in Glassy and Jammed Systems

Tuning pairwise potential can control the fragility of glass-forming liquids: from a tetrahedral network to isotropic soft sphere models

Misaki Ozawa[1,2], Kang Kim[3,4] and Kunimasa Miyazaki[1]

[1] Department of Physics, Nagoya University, Nagoya 464-8602, Japan
[2] Laboratoire Charles Coulomb, UMR 5221 CNRS-Université de Montpellier, Montpellier, France
[3] Department of Physics, Niigata University, Niigata 950-2181, Japan
[4] Division of Chemical Engineering, Graduate School of Engineering Science, Osaka University, Toyonaka, Osaka 560-8531, Japan
E-mail: miyazaki@r.phys.nagoya-u.ac.jp

Received 1 February 2016
Accepted for publication 29 April 2016
Published 1 July 2016

Online at stacks.iop.org/JSTAT/2016/074002
doi:10.1088/1742-5468/2016/07/074002

Abstract. We perform molecular dynamics simulations for a SiO_2 glass former model proposed by Coslovich and Pastore (CP) over a wide range of densities. The density variation can be mapped onto the change of the potential depth between Si and O interactions of the CP model. By reducing the potential depth (or increasing the density), the anisotropic tetrahedral network structure observed in the original CP model transforms into the isotropic structure with the purely repulsive soft-sphere potential. Correspondingly, the temperature dependence of the relaxation time exhibits the crossover from Arrhenius to super-Arrhenius behavior. Being able to control the fragility over a wide range by tuning the potential of a single model system helps us to bridge the gap between the network and isotropic glass formers and to obtain the insight into the underlying mechanism of the fragility. We study the relationship between the fragility and dynamical properties such as the magnitude of the Stokes–Einstein violation and the stretch exponent in the density correlation function. We also demonstrate that the peak of the specific heat systematically shifts as the density increases, hinting that the fragility is correlated with the hidden thermodynamic anomalies of the system.

Keywords: slow relaxation and glassy dynamics, structural glasses (theory)

1742-5468/16/074002+21$33.00

Contents

1. Introduction

The current understanding of the mechanism behind the dramatic slowing down of supercooled liquids near glass transition temperatures still remains far from complete. Although the underlying mechanism of the glass transition is believed to be universal, many dynamical properties of the glass formers are diverse and system-dependent. Among them, the concept of the fragility, or the temperature dependence of the relaxation time and transport coefficients, such as the viscosity and diffusion constant, is one of the most important but least understood problems. For some glass formers, which are called *strong* liquids according to the Angell's classification, the relaxation times obey the Arrhenius law, while others, called *fragile* liquids, show a strong departure from the Arrhenius law in their temperature dependence of the relaxation times [1, 2]. Representative strong glass formers are SiO_2 and GeO_2, whose local molecular configurations are characterized by anisotropic network structures. On the other hand, fragile liquids such as *o*-terphenyl and toluene tend to have more isotropic and compact local structures. The concept of fragility has played a key role in the study of glass transition. Many experimental studies have reported that there exist correlations between the fragility and various thermodynamic, structural, mechanical, and dynamical properties of the glass formers [2]. For example, it has been observed that the entropy and specific heat [1, 3], the elastic constants [4, 5], and the spatially heterogeneous dynamics [6, 7] sensitively depend on the fragility of the systems. Theoretical

doi:10.1088/1742-5468/2016/07/074002

J. Stat. Mech. (2016) 074002

understanding of the fragility, on the other hand, is left at the phenomenological level. Virtually all theoretical scenarios of the glass transition proposed so far, including the Adam–Gibbs theory [8], the random first order transition theory [9], energy landscape picture [10], geometric frustration scenarios [11–14], elastic models [15, 16], soft modes [17], and the dynamic facilitation scenario [18], have their own explanations of the fragility, but the first-principles and microscopic theory to quantitatively describe the fragility is still lacking [10, 19–22].

The difficulty of gaining a unified picture of the fragility from the experimental observations is obviously due to the diversity and complexity of real molecular or polymeric glass formers. The computer simulation is an ideal tool to avoid this difficulty because one can gain all microscopic information of dynamics for relatively simple model systems. Popular glass former models in the simulation studies, such as the soft-sphere (SS) [23] and the Lennard-Jones (LJ) potential liquids [12, 24, 25], are regarded as typical fragile glass formers. On the other hand, strong glass former models with anisotropic networks, where the particles are connected by covalent bonds, such as SiO_2 and GeO_2, have also been studied extensively by simulations [26–29].

There have been several attempts to understand the origin of the fragility systematically by simulations. In many studies, the isotropic potential systems, such as the SS and LJ potentials, have been employed. The fragility has been controlled using various methods, for example, by varying the density or pressure of the system [30–34], by changing the polydispersity [35–37] and the size ratio of the multi-component mixtures [12, 38], by tuning the interaction potential [31, 39, 40], or by truncating the attractive part of the LJ potential [41, 42]. The fragility was also found to be sensitive to many-body interactions which influence the local geometrical frustration [43, 44]. An idea to sort out thermodynamic and purely kinetic contributions to the fragility has been discussed recently [45]. The external parameters such as the impurities [46, 47] and the curvature of the non-Euclidean space [48] have been proposed as a new method to control the fragility. The findings of these studies, however, are still not sufficient to unravel the entire picture of the fragility. Aside from the obvious drawback that the time window which the current simulation can cover is narrow compared with the experiments, one of the obstacles of the computational studies is that the variation of the fragility which the simple glass former models can encompass is small [12, 30–32, 35–42]. Furthermore, the variation of the fragility is often masked by an apparent density-temperature scaling law, which makes it difficult to extract the generic mechanism controlling the fragility [31, 32]. There also remains the nagging question of how to decompose the kinetic and purely thermodynamic contributions of the fragility [45]. Even more important is to bridge the gap between the fragile isotropic systems and the strong network glass formers, which has been studied almost in different arenas in the past. Given these circumstances, it is beneficial to consider a simple model system which can cover a wide range of fragility, spanning from the strongest network glass former down to a very fragile isotropic system, simply by tuning a system parameter.

In this paper, we numerically study a simple model glass former originally introduced by Coslovich and Pastore (CP) as a model strong glass former mimicking SiO_2 [29]. The CP model is a binary mixture of spherical atoms interacting with the isotropic LJ potential with a very strong attraction between Si and O atoms, which allows them to form anisotropic tetrahedral network structures. In this study, the fragility of

J. Stat. Mech. (2016) 074002

the CP model is examined over an extremely wide range of density from the order of unity up to virtually infinity. Varying the density is equivalent to changing the potential depth between Si and O atoms of the CP model. By reducing this potential depth (or increasing the density), the anisotropic tetrahedral network structure observed in the CP model is eventually transformed into an isotropic structure with a purely repulsive soft-sphere potential. Thus, it enables one to control the fragility from strong to fragile systematically.

Here, we summarize the results of this paper. By extensive simulations, dependence of the structure on the density is monitored using the radial distribution functions, the static structure factors, and the coordination numbers. By measuring the temperature dependence of the relaxation time obtained from the density–density time correlation function, we observe that the fragility systematically changes from strong to fragile with the change of the structures. We carefully examine the density-temperature scaling for the temperature dependence of the relaxation time [49–55]. It is confirmed that the relaxation time does not collapse onto a master curve. This implies that the observed fragility variation is not superficial but is due to a qualitative change of the underlying mechanism controlling the slow dynamics. We investigate the correlation between the fragility and several dynamical observables, i.e. the magnitude of the Stokes–Einstein (SE) violation and the exponent of the stretched exponential relaxation of the density correlation function. It has been argued that these observables are manifestations of spatially heterogeneous dynamics, or *the dynamical heterogeneities*, and they are intimately correlated with the fragility [56]. We confirm that more fragile systems show stronger SE violation, whereas a clear-cut correlation between the stretch exponent and the fragility is not observed. Finally, we also discuss the possibility that the fragility is related to the peak position of the specific heat observed in its temperature dependence.

This paper is organized as follows. In section 2, we describe the details of the simulation methods. The numerical results are presented in section 3. Finally, we discuss our results and conclude in section 4.

2. Simulation methods

In this section, we describe the simulation methods.

2.1. The Coslovich–Pastore model

Coslovich and Pastore have introduced a simple SiO_2 (strong glass former) model [29]. Its dynamical and structural properties have been intensively investigated for fixed densities [57–60]. The advantage of this model is its simplicity compared to other established SiO_2 models [26–28]. Although its potential is given by a combination of the SS and LJ potentials, the atoms in the CP model form an anisotropic tetrahedral network structure similar to those of the realistic SiO_2 models [29]. According to [61, 62], there are three conditions for a binary mixture with spherical potential to generate the tetrahedral network structure: (1) The composition ratio is $N_1 : N_2 = 1 : 2$, where

J. Stat. Mech. (2016) 074002

N_1 and N_2 are the number of particles for species 1 and 2, respectively. (2) The potential is non-additive, i.e. the range of the interaction between species 1 and 2 is not a simple sum of their diameters. (3) The attractive interaction between different species is strong. The CP model satisfies these conditions.

The CP model is a binary mixture in three dimensions whose composition ratio is $N_1 : N_2 = 1 : 2$ and the mass ratio is $m_2/m_1 = 0.57$. Species 1 and 2 correspond to Si and O atoms of SiO_2, respectively. The interaction potentials between two particles are given by

$$v_{\alpha_i\beta_j}(r) = \epsilon_{\alpha_i\beta_j}\left\{\left(\frac{\sigma_{\alpha_i\beta_j}}{r}\right)^{12} - C(1-\delta_{\alpha_i\beta_j})\left(\frac{\sigma_{\alpha_i\beta_j}}{r}\right)^{6}\right\}, \tag{1}$$

where C is a constant which was set to unity in the original CP model [29]. We specify the particles by the Roman indices $i, j \in \{1, 2, \cdots, N\}$ and the species by the Greek indices $\alpha_i, \beta_j \in \{1, 2\}$. The parameters are set to $\epsilon_{12}/\epsilon_{11} = 24$, $\epsilon_{22}/\epsilon_{11} = 1$, $\sigma_{22}/\sigma_{11} = 0.85$, and $\sigma_{12}/\sigma_{11} = 0.49$. The last condition warrants that the potential is non-additive, i.e. $\sigma_{12} \neq (\sigma_{11} + \sigma_{22})/2$. $v_{\alpha_i\beta_j}(r)$ is truncated at $r = 2.5\sigma_{\alpha\beta}$. In order to ensure the continuity of the potential, we add a switching function, $S(r)$, up to $r = 3\sigma_{\alpha\beta}$. The switching function connects two points, R_1 and R_2, continuously and is defined as

$$S(r) = \begin{cases} 1 & (0 \leqslant r < R_1), \\ (r-R_2)^2(2r+R_2-3R_1)/(R_2-R_1)^3 & (R_1 \leqslant r < R_2), \\ 0 & (R_2 \leqslant r). \end{cases} \tag{2}$$

We used $R_1 = 2.5\sigma_{\alpha\beta}$ and $R_2 = 3\sigma_{\alpha\beta}$.

2.2. Tuning of the potential depth

In this study, we introduce a parameter C in the second term (the attraction part) of $v_{12}(r)$ in equation (1). C is the strength of the attraction between different species. The depth of the potential well Δ is written in the unit of ϵ_{11} as $\Delta = \epsilon_{12}C^2/4\epsilon_{11}$. Hereafter, we use Δ instead of C. In figure 1, we show $v_{12}(r)$ for various Δ's. $\Delta = 6$ ($C = 1$) corresponds to the original CP model and $\Delta = 0$ ($C = 0$) corresponds to a simple SS potential. Note that the potential for $\Delta = 0$ is slightly different from the conventional SS potential model which has been extensively studied in the past [23], since the range of the interaction is still non-additive. Our model can seamlessly connect the original CP model with the purely repulsive SS potential model. As mentioned above, the atoms with large Δ, i.e. strong attractive interaction, tend to form the tetrahedral network structure. This structure is broken as Δ reduces and eventually the local structure becomes isotropic and compact in the limit of $\Delta = 0$. Mathematically, changing Δ at a constant density ρ is equivalent to changing ρ at a constant Δ. We explain the relation between Δ and ρ using a simple scaling argument, following a similar argument for the SS potential model [63]. The Hamiltonian of the system is written as

$$\frac{H}{k_BT} = \frac{1}{k_BT}\left\{\sum_{i=1}^{N}\frac{\boldsymbol{p}_i^2}{2m_{\alpha_i}} + \sum_{i<j} v_{\alpha_i\alpha_j}(r_{ij})\right\}, \tag{3}$$

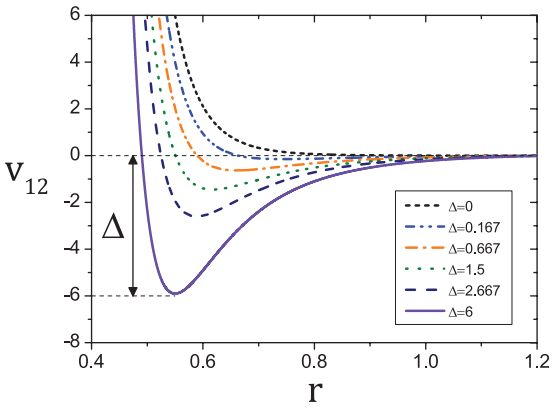

Figure 1. The interaction potential $v_{12}(r)$ between species 1 and 2 for various Δ's from $\Delta = 0$ (top) to $\Delta = 6$ (bottom). $\Delta = 6$ corresponds to the original CP model in [29].

where $k_{\rm B}$, $\boldsymbol{p}_i$, m_{α_i}, and $v_{\alpha_i\alpha_j}(r_{ij})$ are the Boltzmann constant, momentum, mass, and the potential given by equation (1), respectively. Introducing the unit of the length $l = \rho^{-1/3}$, this Hamiltonian can be rewritten as

$$\frac{H}{k_{\rm B}T} = \Gamma^4\left[\sum_{i=1}^{N}\frac{\boldsymbol{p}_i^{*2}}{2m_{\alpha_i}^*} + \sum_{i<j}\epsilon_{\alpha_i\alpha_j}^*\left\{\left(\frac{\sigma_{\alpha_i\alpha_j}^*}{r_{ij}^*}\right)^{12} - C(\rho\sigma_{11}^3)^{-2}(1-\delta_{\alpha_i\alpha_j})\left(\frac{\sigma_{\alpha_i\alpha_j}^*}{r_{ij}^*}\right)^{6}\right\}\right], \tag{4}$$

where $m_{\alpha_i}^*$, $\boldsymbol{p}_{\alpha_i}^*$, $\sigma_{\alpha_i\alpha_j}^*$, and $\epsilon_{\alpha_i\alpha_j}^*$ are reduced parameters scaled by m_1, $m_1 l/\tau_0$, σ_{11}, and ϵ_{11}, respectively. The time unit is defined by $\tau_0 = \{m_1 l^2/\epsilon_{11}(l/\sigma_{11})^{12}\}^{1/2}$. $\Gamma \equiv \rho(\epsilon_{11}/k_{\rm B}T)^{1/4}\sigma_{11}^3$ is a dimensionless parameter commonly used for the SS potential [63]. Note that there exist two dimensionless parameters which control the system: Γ and $C(\rho\sigma_{11}^3)^{-2}$. This means that, for a fixed Γ (or the temperature), changing the density with a fixed C is equivalent to changing C for a fixed density. Therefore, if one chooses the purely LJ system ($C = 1$) with a density ρ_0 as a reference system, one can infer thermodynamic and dynamical properties at arbitrary densities by tuning C for the fixed ρ_0. The mapping from C to ρ is given by $(\rho_0/\rho)^2 = C$, or equivalently in terms of Δ by

$$\left(\frac{\rho_0}{\rho}\right)^2 = \sqrt{\frac{\Delta}{6}}. \tag{5}$$

From this mapping, one can cover the whole range of density up to $\rho = \infty$ by tuning C (or Δ) from a finite value down to 0.

2.3. Details of molecular dynamics simulations

We perform the molecular dynamics (MD) simulations for various Δ's. We use $\Delta = 6$, 2.667, 1.5, 1.042, 0.667, 0.375, 0.167, 0.042 and 0 at a constant density $\rho_0 = 1.655$. The correspondence of various Δ's for a fixed density ρ_0 to various densities for a fixed $\Delta = 6$ is summarized in table 1. By tuning Δ, we explore a wide range of densities from 1.655 up to infinity of the original CP model. The number of the particles is

J. Stat. Mech. (2016) 074002

Table 1. Summary of the parameters, Δ, the corresponding densities ρ, and the temperature range of the present study.

Δ	$\sqrt{\Delta}$	ρ	T	k^*	$T_{\rm onset}$	$T_0^{(\tau_\alpha)}$	$T_0^{(D)}$	T^*	$K^{(\tau_\alpha)}$	$K^{(D)}$
0	0	∞	0.07–0.34	5.8	0.18	0.0548	0.0547	0.085	0.372	0.475
0.042	0.204	5.733	0.06–0.34	5.9	0.16	0.0467	0.0465	0.065	0.357	0.459
0.167	0.408	4.054	0.57–0.34	5.9	0.12	0.0472	0.0461	Non	0.652	0.759
1.042	1.021	2.564	0.065–0.34	5.6	0.14	0.046	0.0456	0.075	0.241	0.286
1.5	1.225	2.341	0.085–0.34	5.5	0.18	0.0599	0.059	0.11	0.2	0.229
2.667	1.633	2.027	0.14–0.6	5.2	0.26	0.0776	0.0793	0.2	0.1	0.126
6	2.449	1.655	0.3–1.25	5.0	0.48	0.161	0.173	0.4	0.087	0.123

Note: The peak position k^* of $S_{11}(k)$, the onset temperature $T_{\rm onset}$ of the two-step relaxation, T_0 obtained by fitting the Vogel–Fulcher–Tammann (VFT) equations from the relaxation time τ_α and diffusion constant D, the peak position T^* of the specific heat, and the fragility index K from τ_α and D are also tabulated.

$N = N_1 + N_2 = 3000$ with $N_1 : N_2 = 1 : 2$. The temperature range in which we perform the simulation are listed in table 1. Hereafter, we use σ_{11}, $\epsilon_{11}/k_{\rm B}$, and $\sqrt{m_1\sigma_{11}^2/\epsilon_{11}}$, as the units of length, time, and temperature, respectively. The micro-canonical MD method with the periodic boundary condition is used to produce the trajectories. A time step $\Delta t = 0.0005$ is chosen throughout this study. For the calculations of the dynamic and thermodynamic quantities, we average over four independent simulation runs.

3. Results

3.1. Structural properties

We first study the structural properties of the CP model for various potential depth Δ. We start with the radial distribution function $g_{\alpha\beta}(r)$. Figure 2 shows $g_{\alpha\beta}(r)$ for each Δ at the lowest temperatures in our simulation which are listed in table 1. For $\Delta = 6$ (see figure 2(d)), $g_{12}(r)$ exhibits a very sharp peak at $r \simeq 0.6\sigma_{11}$ followed by the very broad and small first minimum which persists up to $r \simeq \sigma_{11}$ beyond which the small and broad second peak appears. In contrast, the first peaks of $g_{11}(r)$ and $g_{22}(r)$ are observed at $r \simeq \sigma_{11}$ and $r \simeq \sigma_{22}$, respectively. This indicates that the particles of species 1 and 2 are strongly bonded [29]. As Δ decreases, the first peak of $g_{12}(r)$ gradually decreases and broadens. Concomitantly the height of the first minimum rises to a finite value at around $r \simeq \sigma_{11}$. Finally, at $\Delta = 0$ (see figure 2(a)), the profiles of $g_{11}(r)$, $g_{12}(r)$, and $g_{22}(r)$ become similar to those of typical fragile glass formers such as the SS and LJ binary mixtures [23, 25]. This structural change reflects the fact that the bonds between species 1 and 2 are weakened by decreasing Δ.

To understand the effect of Δ on the structure in more detail, we calculate the coordination number $z_{\alpha\beta}$. $z_{\alpha\beta}$ is the averaged number of the β particles in the first neighbor shell of the α particle and defined by

$$z_{\alpha\beta} = \rho_\beta \int_0^{r^*_{\alpha\beta}} {\rm d}r 4\pi r^2 g_{\alpha\beta}(r), \tag{6}$$

J. Stat. Mech. (2016) 074002

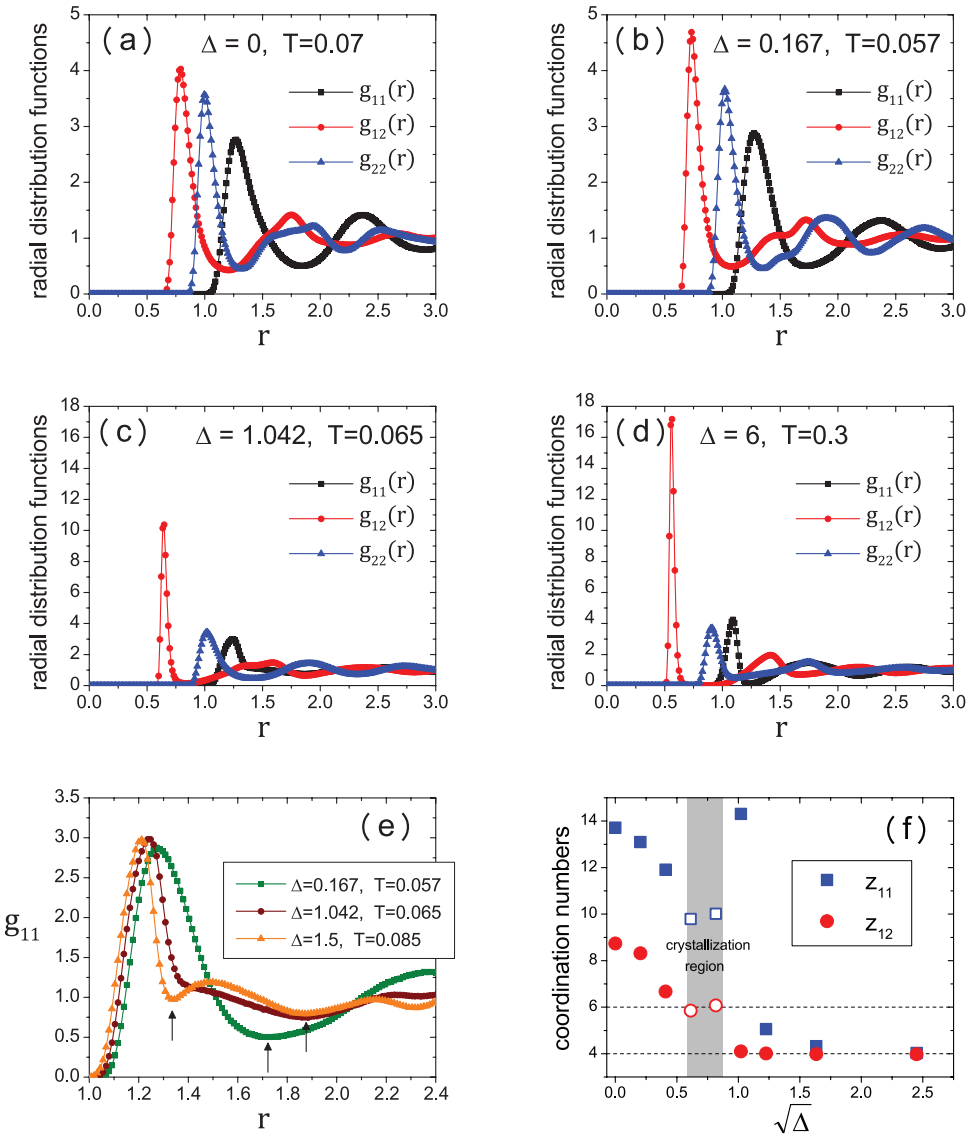

Figure 2. (a)–(d) The radial distribution functions, $g_{11}(r)$, $g_{12}(r)$, and $g_{22}(r)$, for several Δ's. The data for the lowest temperature for each Δ are shown. (e) $g_{11}(r)$ for several Δ's around 1. The vertical arrows are the position r_{11}^{*} of the first minimum in $g_{11}(r)$. (f) The coordination numbers z_{11} and z_{12} as a function of $\sqrt{\Delta}$. Data for the lowest temperatures are shown for each Δ. The open symbols are the results for the crystalline structure.

where ρ_β is the number density of species β and $r_{\alpha\beta}^{*}$ is the position of the first minimum of $g_{\alpha\beta}(r)$. In particular, z_{11} and z_{12} are useful to characterize the tetrahedral network structure. In SiO_2, a single Si atom (species 1) is surrounded by four oxygen atoms (species 2), thus, $z_{11} = 4$, $z_{12} = 4$, and $z_{21} = 2$. In figure 2(f), we show z_{11} and z_{12} at the lowest temperatures for several Δ's. We use $\sqrt{\Delta}$ instead of Δ as the horizontal axis for the sake of visual clarity. At $\Delta = 6$ ($\sqrt{\Delta} \simeq 2.449$), we obtain $z_{11} = 4$ and $z_{12} = 4$, corresponding to the perfect tetrahedral network structure [29]. As Δ decreases, both z_{11} and z_{12} increase. Eventually, we observe $z_{11} \simeq 14$ and $z_{12} \simeq 9$ at $\Delta = 0$. This indicates

that the tetrahedral network structure is broken and that the local configuration of the system becomes more isotropic and compact. We find that, in a narrow range of Δ, $0.375 \leqslant \Delta \leqslant 0.667$ (or $0.612 \lesssim \sqrt{\Delta} \lesssim 0.816$), the system crystallizes at low temperatures. Some of the samples in our simulation runs also crystallized at the lowest T at $\Delta = 0.167$ and 1.042, when we carried out the simulation for a very long time ($t \gtrsim 10^6$). We show the results for the crystalline state by open symbols in figure 2(f). We confirm by carefully inspecting the real space snapshots that the systems crystallize completely over the entire simulation box. The coordination numbers for the crystallized samples are $z_{12} = 6$ and $z_{11} = 10$. This suggests that the observed crystalline structure is of Stishovite type. Indeed, it has been reported that SiO_2 forms the Stishovite crystal under very high pressures [64]. We remark that an exceptionally large value of $z_{11} \gtrsim 14$ at $\Delta = 1.042$ ($\sqrt{\Delta} \simeq 1.021$) is due to the ambiguity of defining the first coordination shell. As shown in figure 2(e), the profile of $g_{11}(r)$ is broadened around $\Delta \simeq 1$, which makes it difficult to define r_{11}^* clearly. Thus, $\Delta \simeq 1$ can be regarded as the crossover regime from the network dominated region to the isotropic/compact structure region.

Next, we calculate the static structure factor $S_{\alpha\beta}(k)$. We show $S_{\alpha\beta}(k)$ at the lowest temperatures in figure 3 for several Δ's. At $\Delta = 6$, the maximal peaks are observed around $k \simeq 8$ in all components of $S_{\alpha\beta}(k)$. These peaks originate from the tetrahedral structure whose bond length is estimated to be $2\pi/k \simeq 0.79$. We also find weaker peaks at smaller wave numbers around $k \simeq 5$. This is the so-called first sharp diffraction peak (FSDP) [65], which is known as an indication of the medium-range order of the length scale larger than the neighbor shell. In particular, the FSDP has been attributed to the formation of the hierarchical clusters of the tetrahedra with larger lengths [66]. When the potential depth Δ is reduced, these two peaks merge to a single peak. This result implies that the hierarchical tetrahedral structures disappear gradually as Δ is decreased. At $\Delta \lesssim 1$, the shape of the static structure factors are analogous to those observed in typical fragile glass formers such as the SS and LJ binary mixtures [67, 68].

3.2. Dynamical properties

As demonstrated above, the tetrahedral network structures are broken when the potential depth Δ is reduced to zero. In this section, we analyze the dynamical properties of the CP model. Specifically, the Δ dependence of the fragility is quantified.

First, we calculate the self part of the intermediate scattering function $F_s(k, t)$ for species 1 defined by

$$F_s(k, t) = \frac{1}{N_1} \sum_{i=1}^{N_1} \left\langle e^{-i\boldsymbol{k}\cdot(\boldsymbol{r}_i(t) - \boldsymbol{r}_i(0))} \right\rangle, \tag{7}$$

where $\boldsymbol{r}_i(t)$ denotes the position of the ith particle at time t. In figure 4, we show the temperature dependence of $F_s(k, t)$ for several Δ's. The wave number $k = |\boldsymbol{k}|$ is chosen at the peak position k^* of the static structure factor, $S_{11}(k)$ (see figure 3). The values of k^* are listed in table 1. At high temperatures, $F_s(k, t)$ shows the exponential decay with the short relaxation time but, at low temperatures, dynamics dramatically slows down and $F_s(k, t)$ exhibits a two-step relaxation. This is the sign of the onset of the glassy dynamics.

J. Stat. Mech. (2016) 074002

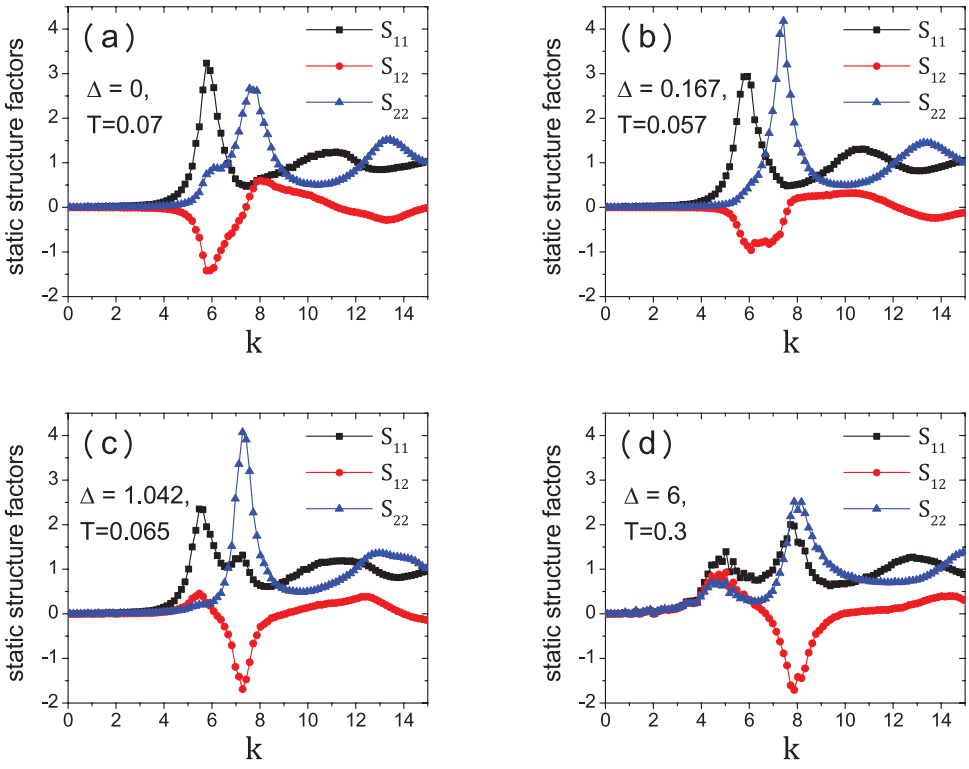

Figure 3. (a)–(d) The static structure factors, $S_{11}(k)$, $S_{12}(k)$, and $S_{22}(k)$, for several Δ's. The results for the lowest temperatures of our simulations are shown.

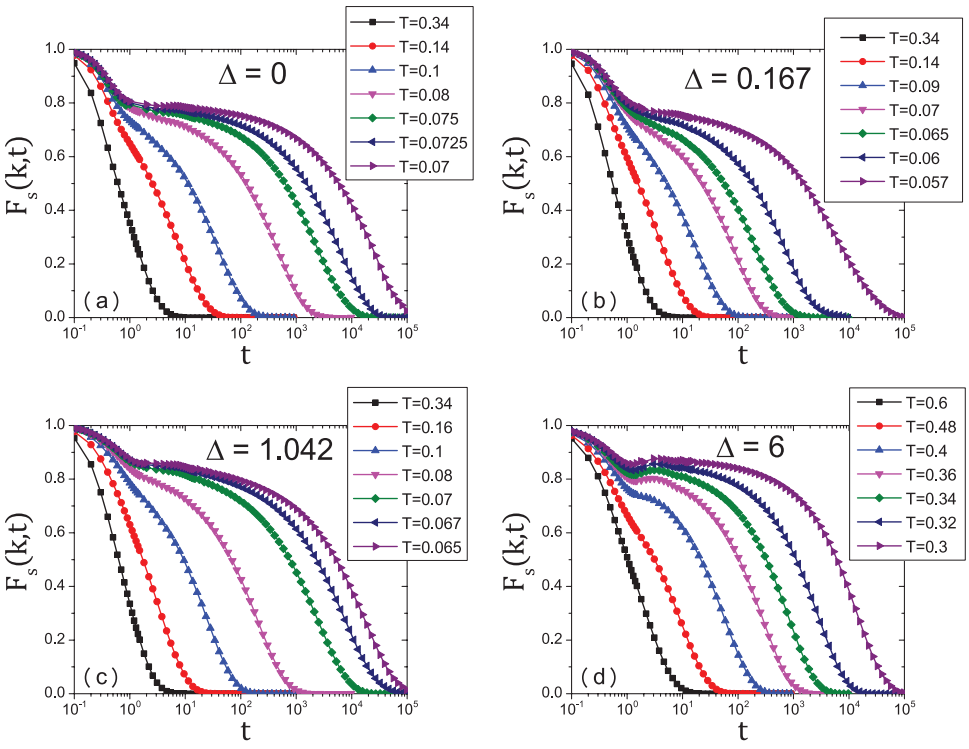

Figure 4. (a)–(d) The temperature variation of the self part of the intermediate scattering function for species 1 for several Δ's.

We define the relaxation time τ_α by $F_s(k, \tau_\alpha) = e^{-1}$. We fit the observed τ_α by the VFT equation:

$$\tau_\alpha \sim \exp\left[\frac{1}{K(T/T_0 - 1)}\right], \tag{8}$$

where T_0 and K are the fitting parameters. The parameter K is referred to as the fragility index which is regularly used to quantify the degree of the super-Arrhenius temperature dependence [30]. The larger (smaller) values of K correspond to the fragile (strong) glass formers. In this study, the VFT fitting is applied below $T_{\rm onset}$, where the two-step relaxation for $F_s(k, t)$ sets in. $T_{\rm onset}$ for each Δ is presented in table 1. We show the temperature dependence of τ_α for several Δ's in figure 6(a). The temperature T is scaled by T_0. It is clearly seen that the results for $\Delta = 2.667$ and $\Delta = 6$ follow the Arrhenius law at low temperatures [29]. For smaller Δ's, the temperature dependence of τ_α deviates from the Arrhenius behavior. In other words, the system changes from strong to fragile glass formers with decreasing Δ.

We also quantify the self diffusion constant D_α ($\alpha \in \{1, 2\}$) from the long-time behavior of the mean squared displacement (MSD). The MSD for species 1 is presented in figure 5. Figure 6(b) shows $(D_1/T)^{-1}$ as a function of T_0/T.

The Δ dependence of the fragility index K is demonstrated in figure 7. At $\Delta = 6$, the value of K is small ($K \approx 0.1$), which is consistent with the results of the previous study [29]. As shown in figure 7, K increases with a decrease in Δ. At $\Delta = 1.042$ ($\sqrt{\Delta} = 1.021$), K exceeds the value of the KA mixture, which is a typical fragile glass former ($K \simeq 0.2$) [40]. We address the fact that the observed fragility index covers a wide range from $K = 0.087$ to 0.652. In particular, the maximal value of $K = 0.652$ at $\Delta = 0.167$ is comparable with those of the most fragile glass formers studied in the simulations [14, 69]. K is also obtained by using the VFT equation for $(D_1/T)^{-1}$. The results are plotted with filled circles in figure 7. Although K obtained from $(D_1/T)^{-1}$ are larger than those obtained from τ_α for all Δ's, the overall behavior is qualitatively the same. We remark that the increase of the fragility index with an increase in density has been reported for the BKS model [28], although the investigated densities were limited [70].

The observation that the system becomes the most fragile (K becomes the largest) just next to the crystalline state may be related to the frustration scenario which claims that the fragility is controlled by the frustration against crystallization [71]. In fact, it has been reported that the system with a weaker frustration against crystallization tends to have larger fragility indices [36, 43]. Further investigation of the dynamics around this Stishovite-like crystallization regime would be valuable to verify the scenario.

In order to characterize the difference of dynamics between the strong (large Δ) and fragile (small Δ) regimes, we evaluate the ratio of the diffusion constants D_2/D_1 between species 1 and 2. In the experiments for SiO_2, it has been reported that the diffusion of Si and O atoms decouples at low temperatures and the ratio of the diffusion constants for Si and O, D_O/D_{Si}, increases with a decrease in temperature [72]. Similar behavior has also been demonstrated in simulations [73, 74]. As mentioned in [74], this decoupling is attributed to the rotational motion of the oxygen atom in the tetrahedral structure. In figure 8, we show D_2/D_1 as a function of τ_α for several Δ's. At $\Delta = 6$,

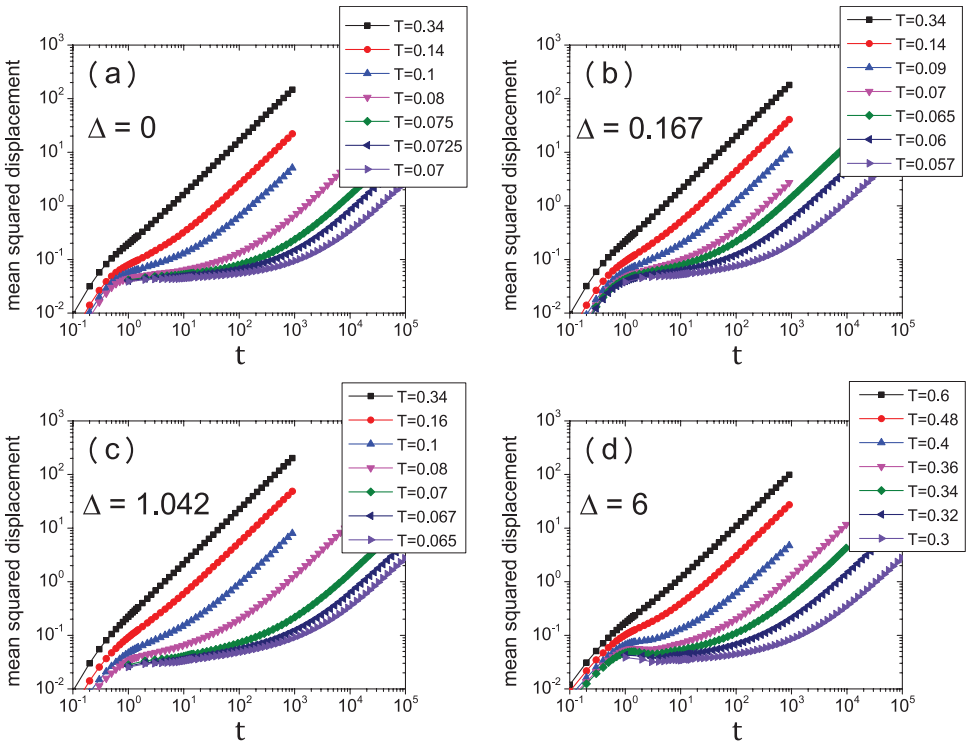

Figure 5. (a)–(d) The temperature variation of the mean squared displacement for species 1 for several Δ's.

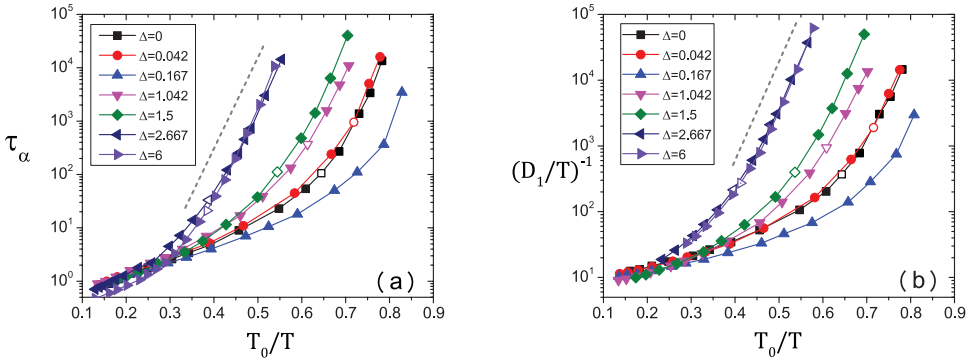

Figure 6. The Arrhenius plots of the relaxation time (a) and of the diffusion constant for species 1 (b) as a function of the inverse temperature $1/T$. In both plots, the temperature is scaled by T_0, a fitting parameter of the VFT equation. The open symbols are the position of T^* at which the specific heat shows the peak (see figure 12). The dashed straight lines indicate the Arrhenius temperature dependence.

D_2/D_1 increases with increasing τ_α (with a decrease in temperature). This is consistent with the results for the original CP model [29]. As Δ decreases, the variation of D_2/D_1 becomes milder and eventually becomes almost a flat line at $\Delta = 0.167$. As Δ decreases further below $\Delta = 0.167$, the trend is reversed and D_2/D_1 becomes an increasing function of τ_α again and the slope keeps increasing until Δ reaches 0, where the slope becomes maximum. The degree of the decoupling at $\Delta = 0$, which corresponds to the

J. Stat. Mech. (2016) 074002

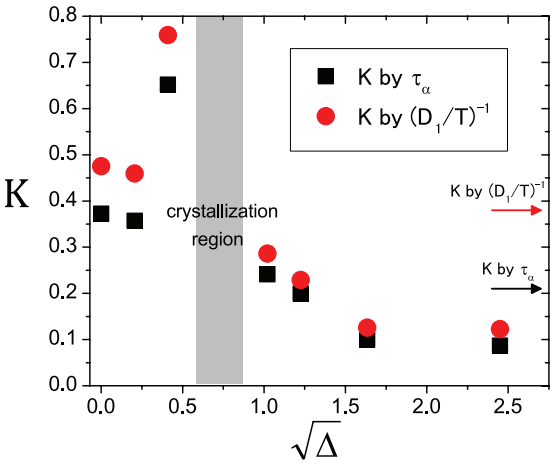

Figure 7. The fragility index K as a function of Δ. The results of the VFT fitting by τ_α and $(D_1/T)^{-1}$ are shown as the squares and circles, respectively. The results of the Kob–Andersen (KA) mixture from Sengupta *et al* [40] are shown by the horizontal arrows. The gray shaded area indicates the region where we observe crystallization at lower temperatures.

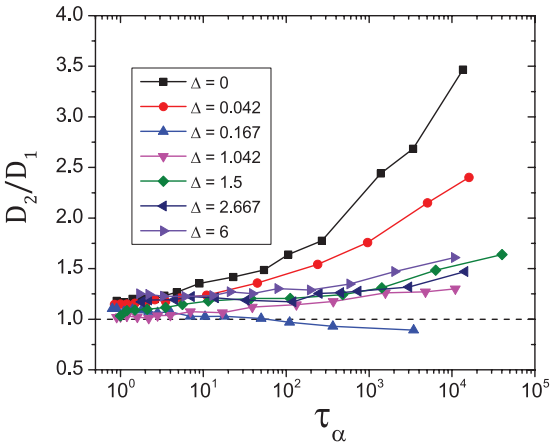

Figure 8. The ratio of the diffusion constants D_2/D_1 as a function of τ_α for several Δ's.

SS model, is even larger than that of the network glass former at $\Delta = 6$. Similar strong decoupling between D_1 and D_2 has been reported for the conventional SS model [75]. This non-monotonic Δ dependence of D_2/D_1 is another signature that the dynamics of the CP model are changed qualitatively by tuning the potential depth Δ. It is natural to expect that the underlying mechanisms behind the strong decoupling of D_1 and D_2 at the two extreme ends of $\Delta = 0$ and 6 are completely different. It would be worthwhile seeking the origin of this strong decoupling for $\Delta = 0$.

3.3. Absence of the density-temperature scaling

The density-temperature (DT) scaling is a useful way to single out the parameter which controls the thermodynamic and dynamical properties of liquids. The simplest example

is the inverse power law (IPL) potential, $v(r) \sim r^{-n}$, where the DT scaling exactly holds and the system is characterized by a single parameter, $\rho^{\frac{n}{d}}/T$, where d is the spatial dimension [63]. It has been known that a broad class of liquids can be scaled by a single parameter ρ^{γ}/T, where γ is a constant [50, 52–55]. It has been argued that the DT scaling holds if there is a strong correlation between the virial W and the potential energy U. The liquids for which the correlation between W and U is more than 90%, are called *strongly correlating or Roskilde-simple liquids* [52–55]. Since the CP model with $\Delta = 0$ is a purely IPL system, the DT scaling exactly holds. On the other hand, the previous study has demonstrated that at $\Delta = 6$ (non-IPL system), the correlation coefficient between W and U is less than 10% (non-strongly correlating liquid), thus the DT scaling does not hold [76]. Consequently, the validity of the DT scaling for the CP model varies depending on Δ.

There is another type of DT scaling where it is convenient to characterize the dynamical quantities such as the relaxation time $\tau_\alpha(\rho, T)$. It has been argued that $\tau_\alpha(\rho, T)$ for many liquids is scaled by the characteristic time and energy at high temperatures, $\tau_\infty(\rho)$ and $E_\infty(\rho)$. $\tau_\infty(\rho)$ and $E_\infty(\rho)$ are determined by fitting $\tau_\alpha(\rho, T)$ at high temperatures using the Arrhenius law:

$$\tau_\alpha(\rho, T) \simeq \tau_\infty(\rho) \exp[E_\infty(\rho)/T]. \tag{9}$$

This scaling has also been demonstrated to work well in many supercooled liquids and polymer systems [49–51].

As mentioned in section 1, the density or pressure dependence of the fragility has been studied in various systems [30–33]. However, some of those results can be collapsed onto a master curve using the DT scaling, which means that the observed variation of the fragility is only superficial with no physical significance [31, 32].

Here, we examine the DT scaling using equation (9), for the relaxation time $\tau_\alpha(\Delta, T)$ of the CP model. In figure 9, $\tau_\alpha(\Delta, T)$ scaled by $\tau_\infty(\Delta)$ is plotted as a function of $E_\infty(\Delta)/T$. In this figure, the potential depth Δ is used instead of the density ρ. At the small Δ regime, the relaxation times are collapsed onto a master curve, whereas they systematically deviate from the master curve as Δ increases. This result eloquently demonstrates that the dynamical properties of the CP model do not follow the DT scaling. From these results, it is concluded that the observed variation of the fragility is not superficial but it is a genuine manifestation of the changeover of the physical mechanism.

3.4. Stokes–Einstein violation and stretch exponent

The advantage of the CP model is that the correlation of physical quantities with the fragility can be studied systematically in a single system over a wide range of fragility. In particular, it enables one to examine the much debated issues on the relation of fragility with dynamical properties, such as the SE violation and the stretched exponential relaxation. In normal liquids, it is expected that the SE relation, $D\eta/T \propto \text{const.}$ holds, where D and η are the diffusion constant and viscosity, respectively. However, the SE relation is violated in most supercooled liquids near the glass transition temperature. This SE violation is often regarded as a manifestation of the spatially heterogeneous dynamics, or *the dynamical heterogeneities* [56]. Previously, the SE violation of the

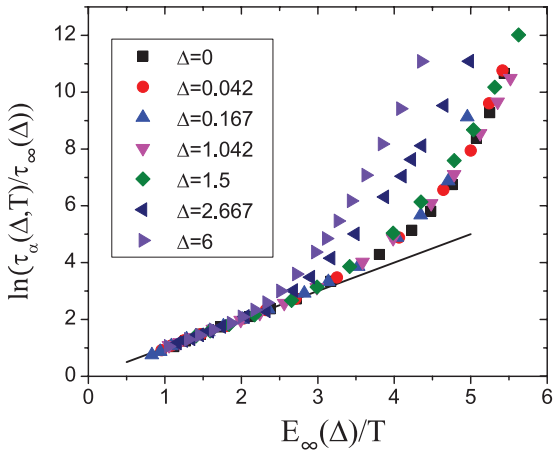

Figure 9. The density-temperature scaling for the relaxation time $\tau_\alpha(\Delta, T)$ scaled by $\tau_\infty(\Delta)$ as a function of $E_\infty(\Delta)/T$. The straight line represents equation (9).

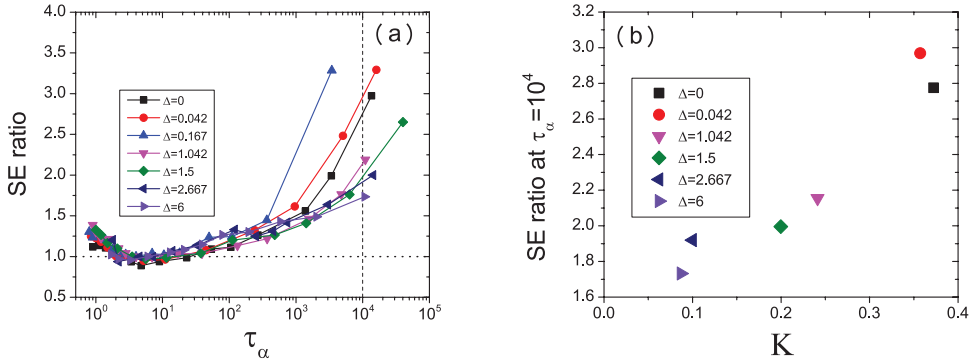

Figure 10. (a) The SE ratio as a function of τ_α. The vertical dashed line corresponds to $\tau_\alpha = 10^4$. (b) The SE ratio at $\tau_\alpha = 10^4$ as a function of K.

original CP model ($\Delta = 6$) has been investigated [59, 60]. These studies highlight the qualitative difference between the CP model ($\Delta = 6$) and other fragile glass formers in their dynamical behavior [77]. The aim of this section is to elucidate the dependence of the SE violation on fragility in a systematic way.

In figure 10(a), we show the SE ratio, $D_1(T)\tau_\alpha(T)/D_1(T_{\rm onset})\tau_\alpha(T_{\rm onset})$, normalized by the values at $T_{\rm onset}$, as a function of τ_α. For all Δ's, the SE relation is violated, i.e. the SE ratio increases with an increase in τ_α (or a decrease in temperature). We remark that the deviation of the SE ratio at high temperatures (small τ_α) is an artifact caused by the use of τ_α instead of η/T [59, 78, 79]. Dependence of the SE violation on fragility is shown in figure 10(b). Here we plot the SE ratio at low temperatures (at $\tau_\alpha = 10^4$) against the fragility index K. A clear correlation between the SE violation and the fragility is observed, that is, the more fragile systems tend to exhibit stronger SE violation.

Next, we study the stretch exponent $\beta_{\rm KWW}$ of the nonexponential relaxation observed in the density correlation function. Experimental studies have shown that the fragile systems tend to have smaller stretch exponents than the strong systems [6, 7]. Some theories explain this observation [80], while others argue that there is no direct correlation between the fragility and $\beta_{\rm KWW}$ [81, 82].

J. Stat. Mech. (2016) 074002

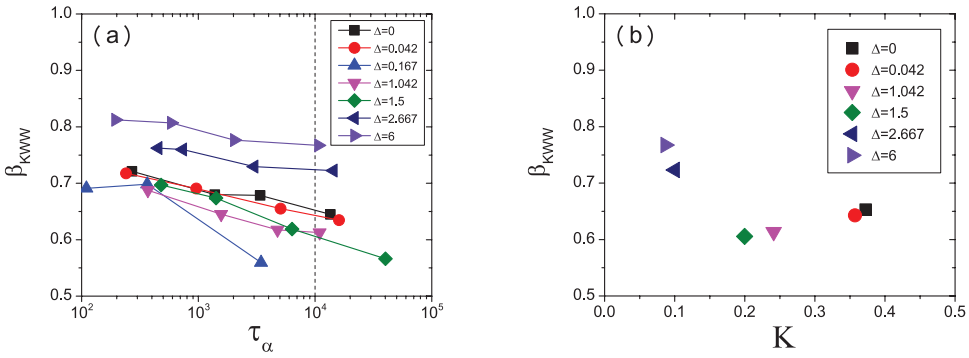

Figure 11. (a) The stretch exponent β_{KWW} as a function of τ_α. The vertical dashed line corresponds to $\tau_\alpha = 10^4$. (b) β_{KWW} at $\tau_\alpha = 10^4$ as a function of K.

Here, we show the fragility dependence of the stretch exponents of the CP model. We determine β_{KWW} from $F_{\mathrm{s}}(k, t)$ using the following fitting function,

$$F_{\mathrm{s}}(k, t) = (1 - f_{\mathrm{c}}) \exp[-(t/\tau_{\mathrm{s}})^2] + f_{\mathrm{c}} \exp[-(t/\tau_{\mathrm{l}})^{\beta_{\mathrm{KWW}}}], \tag{10}$$

where f_{c}, τ_{s} and τ_{l} are fitting parameters [78]. Figure 11(a) shows β_{KWW} as a function of τ_α. For all Δ's, β_{KWW} decreases gradually with an increase in τ_α (a decrease in temperature). In figure 11(b), we plot β_{KWW} at $\tau_\alpha = 10^4$ as a function of K. Surprisingly, we observe no clear correlation between the fragility and β_{KWW}, although β_{KWW} becomes somewhat larger at a strong-liquid regime of $\Delta = 2.667$ and 6. This observation is not inconsistent with the argument in [82]. A similar trend has been reported for the harmonic sphere model [33].

3.5. Relationship with specific heat peak

Finally, we discuss the possible relationship between the thermodynamic properties and the fragility variation observed in the CP model. Several simulation studies using the BKS model [28] for SiO_2 have demonstrated that there exists the so-called fragile-to-strong (FS) crossover; the temperature dependence of the relaxation time changes from super-Arrhenius (fragile) to Arrhenius (strong) behavior with a decrease in temperature [73, 83, 84]. It has been argued that this FS crossover is related to a thermodynamic anomaly signaled by the appearance of the peak of the specific heat [83–85] which tends to shift to lower temperatures if the density is increased [83, 84, 86]. This anomaly might be connected to a hidden thermodynamic singularity such as the liquid–liquid transition, but the overall picture is still unclear. Under these circumstances, it is of great interest to examine whether the FS crossover and the shift of the specific heat are also observed in the CP model by tuning the potential depth Δ.

The specific heat is calculated by $c_V = \frac{1}{N}\frac{\partial U}{\partial T}$. Figure 12 shows the temperature dependence of c_V for various potential depths Δ. The temperature T is normalized by the onset temperature T_{onset}. As observed, there exists the broad but clear peak of c_V at a finite temperature T^* for all Δ's except for $\Delta = 0.167$. We cannot access the lower temperatures for $\Delta = 0.167$ because the system crystallizes. The temperature T^* for each Δ is listed in table 1. We find that T^* shifts to lower temperatures with decreasing Δ (increasing the density).

J. Stat. Mech. (2016) 074002

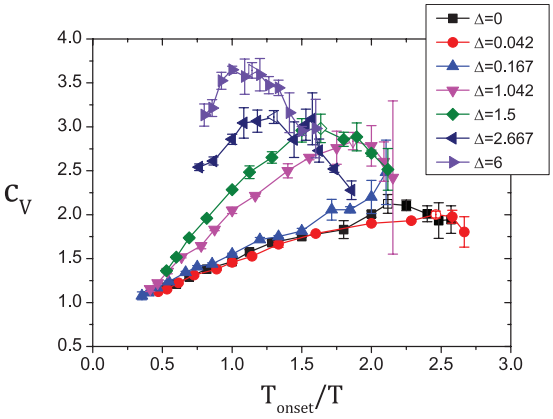

Figure 12. The specific heat as a function of the inverse temperature for several Δ's. The temperature is scaled by $T_{\rm onset}$. The open symbols are the positions of the peak.

Contrary to the distinct peaks of the specific heat, the FS crossover is harder to detect in the simulation data. Due to the limited range of the temperature in the Arrhenius plot of figure 6, one hardly observes any sort of distinct crossover. In this figure, we marked the temperatures at which the peak of the specific heat are observed with the empty symbols as a guide for the eyes. For the data of $\Delta = 2.667$ and 6, it is not impossible to fit the data of τ_α with the Arrhenius and super-Arrhenius laws on the low and high temperature sides across T^*, but the fitting range is too narrow to call it convincing. Similar fitting was also possible for smaller values of Δ's, but it is less trustworthy. Therefore, it would be fair to say that the existence of the correlation between the FS crossover and the peak of the specific heat is not conclusive in current numerical simulations [83, 84, 86]. More extensive simulations are required to clarify the relation between the FS crossover and the specific heat peak.

4. Summary and discussion

We have numerically investigated the CP model by tuning the depth of the potential Δ. Changing Δ corresponds to changing the density of the system. This approach has enabled us to perform simulations over a wide range of densities from the order of unity up to infinity. From the radial distribution functions, the coordination numbers, and the static structure factors, we found that the anisotropic tetrahedral network structures are broken and then the isotropic structures are formed by decreasing Δ (or increasing the density). We have also calculated various dynamical quantities such as the relaxation time and diffusion constant. These calculations have revealed that their temperature dependence seamlessly changes from Arrhenius to super-Arrhenius behavior. We also confirmed that the temperature dependence of the dynamics is not collapsed by the DT scaling, assuring us that the observed fragility change is not a consequence of the trivial density scaling but is due to the generic change of the mechanism of the glassy dynamics. We have studied the relationship between the fragility and two dynamical quantities, the magnitude of the SE violation and the stretch

exponent of the density correlation function. The magnitude of the SE violation, which is believed to be a manifestation of the dynamical heterogeneities, correlates well with the fragility of the CP model. On the contrary, the clear correlation between fragility and the stretch exponent has not been observed. Finally, the peak of the specific heat and the possible correlation with the FS crossover have been argued. The peak has been observed in the temperature dependence of the specific heat for most Δ's in the CP model. In addition, its peak position shifts to lower temperatures with a decrease in the potential depth Δ (or an increase in density). These observations are related to the recent numerical results obtained in the BKS model [83, 84, 86]. However, it was difficult to identify the FS crossover temperature from the relaxation times because the simulation time windows are too narrow and we conclude that the correlation between the FS crossover and thermodynamic anomaly is still elusive. Further numerical investigation is required.

We address the fact that the CP model exhibits a very broad variation of the fragility, the highest and lowest values of which are comparable to those of the most fragile and strongest liquids studied numerically in the past, and that it can serve as an ideal benchmark for the numerical study of fragility. Note that the harmonic sphere model also shows a very wide variation of the fragility as the density is varied [33, 87]. This model also does not satisfy the DT scaling. However, it should be emphasized that this model is qualitatively different from the CP model. In the harmonic sphere model, the potential is truncated at a certain cutoff distance. At low densities, the model becomes effectively a hard sphere system. Therefore, the temperature and energy are not relevant but, instead, the pressure or density become the controlling thermodynamic parameters. This means that at low densities the temperature dependence of the relaxation time is trivially Arrhenius, whereas at higher densities, the temperature plays a pivotal role, leading to more diverging (or fragile) behavior. For the CP model, on the contrary, the temperature plays a role as a relevant control parameter for all densities and the fragility is continuously controlled.

There are other physical quantities that are expected to be related to fragility [2]: the excess entropy [3], the elastic constants [4, 5], the non-ergodicity parameter [88], the boson peak frequency [5], and the temperature dependence of the microscopic structure [89]. In addition, the relationship between the fragility and the dynamical heterogeneities is a topic which has attracted much attention recently [58, 90, 91]. The comprehensive information on the correlation of these properties with fragility will be obtained from the systematic study of the CP model by tuning a single parameter Δ. Further investigations along this line are currently underway.

Acknowledgments

We thank D Coslovich, A Ikeda, H Ikeda, and T Kawasaki for helpful discussions. M O acknowledges financial support by Grant-in-Aid for Japan Society for the Promotion of Science Fellows (26.1878). This work is partially supported by KAKENHI Grants No. 24340098 (K M), 25103005 'Fluctuation & Structure' (K M), 25000002 (K M), 26400428 (K K), 16H00829 'Soft Molecular Systems' (K K), and 26400428 (K K). K M also thanks the JSPS Core-to-Core program. The numerical calculations have been performed at the Research Center for Computational Science, Okazaki, Japan.

References

[1] Angell C A 1995 Formation of glasses from liquids and biopolymers *Science* **267** 1924
[2] Lindsay Greer A, Kenneth F K and Srikanth S 2014 *Fragility of Glass-Forming Liquids* (New Delhi: Hindustan Book Agency)
[3] Martinez L M and Angell C 2001 A thermodynamic connection to the fragility of glass-forming liquids *Nature* **410** 663
[4] Novikov V and Sokolov A 2004 Poisson's ratio and the fragility of glass-forming liquids *Nature* **431** 961
[5] Novikov V, Ding Y and Sokolov A 2005 Correlation of fragility of supercooled liquids with elastic properties of glasses *Phys. Rev.* E **71** 061501
[6] Böhmer R, Ngai K, Angell C and Plazek D 1993 Nonexponential relaxations in strong and fragile glass formers *J. Chem. Phys.* **99** 4201
[7] Niss K, Dalle-Ferrier C, Tarjus G and Alba-Simionesco C 2007 On the correlation between fragility and stretching in glass-forming liquids *J. Phys.: Condens. Matter* **19** 076102
[8] Adam G and Gibbs J H 1965 On the temperature dependence of cooperative relaxation properties in glass-forming liquids *J. Chem. Phys.* **43** 139
[9] Xia X and Wolynes P G 2000 Fragilities of liquids predicted from the random first order transition theory of glasses *Proc. Natl Acad. Sci. USA* **97** 2990
[10] Debenedetti P G and Stillinger F H 2001 Supercooled liquids and the glass transition *Nature* **410** 259
[11] Tarjus G, Kivelson D and Viot P 2000 The viscous slowing down of supercooled liquids as a temperature-controlled super-Arrhenius activated process: a description in terms of frustration-limited domains *J. Phys.: Condens. Matter* **12** 6497
[12] Coslovich D and Pastore G 2007 Understanding fragility in supercooled Lennard-Jones mixtures. I. Locally preferred structures *J. Chem. Phys.* **127** 124504
[13] Tanaka H 2012 Bond orientational order in liquids: towards a unified description of water-like anomalies, liquid–liquid transition, glass transition, and crystallization *Eur. Phys. J.* E **35** 1
[14] Royall C P, Malins A, Dunleavy A J and Pinney R 2015 Strong geometric frustration in model glassformers *J. Non-Cryst. Solids* **407** 34
[15] Dyre J C 2006 Colloquium: the glass transition and elastic models of glass-forming liquids *Rev. Mod. Phys.* **78** 953
[16] Krausser J, Samwer K H and Zaccone A 2015 Interatomic repulsion softness directly controls the fragility of supercooled metallic melts *Proc. Natl Acad. Sci. USA* **112** 13762
[17] Yan L, Düring G and Wyart M 2013 Why glass elasticity affects the thermodynamics and fragility of supercooled liquids *Proc. Natl Acad. Sci. USA* **110** 6307
[18] Garrahan J P and Chandler D 2003 Coarse-grained microscopic model of glass formers *Proc. Natl Acad. Sci. USA* **100** 9710
[19] Cavagna A 2009 Supercooled liquids for pedestrians *Phys. Rep.* **476** 51
[20] Berthier L and Biroli G 2011 Theoretical perspective on the glass transition and amorphous materials *Rev. Mod. Phys.* **83** 587
[21] Binder K and Kob W 2011 *Glassy Materials and Disordered Solids: an Introduction to their Statistical Mechanics* (Singapore: World Scientific)
[22] Royall C P and Williams S R 2015 The role of local structure in dynamical arrest *Phys. Rep.* **560** 1
[23] Bernu B, Hansen J, Hiwatari Y and Pastore G 1987 Soft-sphere model for the glass transition in binary alloys: pair structure and self-diffusion *Phys. Rev.* A **36** 4891
[24] Wahnström G 1991 Molecular-dynamics study of a supercooled two-component Lennard-Jones system *Phys. Rev.* A **44** 3752
[25] Kob W and Andersen H C 1995 Testing mode-coupling theory for a supercooled binary Lennard-Jones mixture I: the van Hove correlation function *Phys. Rev.* E **51** 4626
[26] Woodcock L, Angell C and Cheeseman P 1976 Molecular dynamics studies of the vitreous state: simple ionic systems and silica *J. Chem. Phys.* **65** 1565
[27] Tsuneyuki S, Tsukada M, Aoki H and Matsui Y 1988 First-principles interatomic potential of silica applied to molecular dynamics *Phys. Rev. Lett.* **61** 869
[28] van Beest B, Kramer G J and Van Santen R 1990 Force fields for silicas and aluminophosphates based on *ab initio* calculations *Phys. Rev. Lett.* **64** 1955
[29] Coslovich D and Pastore G 2009 Dynamics and energy landscape in a tetrahedral network glass-former: direct comparison with models of fragile liquids *J. Phys.: Condens. Matter* **21** 285107
[30] Sastry S 2001 The relationship between fragility, configurational entropy and the potential energy landscape of glass-forming liquids *Nature* **409** 164

J. Stat. Mech. (2016) 074002

[31] De Michele C, Sciortino F and Coniglio A 2004 Scaling in soft spheres: fragility invariance on the repulsive potential softness *J. Phys.: Condens. Matter* **16** L489
[32] Sengupta S, Schrøder T B and Sastry S 2013 Density-temperature scaling of the fragility in a model glass-former *Eur. Phys. J.* E **36** 1
[33] Berthier L and Witten T A 2009 Compressing nearly hard sphere fluids increases glass fragility *Europhys. Lett.* **86** 10001
[34] Wang L, Duan Y and Xu N 2012 Non-monotonic pressure dependence of the dynamics of soft glass-formers at high compressions *Soft Matter* **8** 11831
[35] Kawasaki T, Araki T and Tanaka H 2007 Correlation between dynamic heterogeneity and medium-range order in two-dimensional glass-forming liquids *Phys. Rev. Lett.* **99** 215701
[36] Kawasaki T and Tanaka H 2010 Structural origin of dynamic heterogeneity in three-dimensional colloidal glass formers and its link to crystal nucleation *J. Phys.: Condens. Matter* **22** 232102
[37] Abraham S E, Bhattacharrya S M and Bagchi B 2008 Energy landscape, antiplasticization, and polydispersity induced crossover of heterogeneity in supercooled polydisperse liquids *Phys. Rev. Lett.* **100** 167801
[38] Kurita R and Weeks E R 2010 Glass transition of two-dimensional binary soft-disk mixtures with large size ratios *Phys. Rev.* E **82** 041402
[39] Bordat P, Affouard F, Descamps M and Ngai K 2004 Does the interaction potential determine both the fragility of a liquid and the vibrational properties of its glassy state? *Phys. Rev. Lett.* **93** 105502
[40] Sengupta S, Vasconcelos F, Affouard F and Sastry S 2011 Dependence of the fragility of a glass former on the softness of interparticle interactions *J. Chem. Phys.* **135** 194503
[41] Berthier L and Tarjus G 2009 Nonperturbative effect of attractive forces in viscous liquids *Phys. Rev. Lett.* **103** 170601
[42] Coslovich D 2011 Locally preferred structures and many-body static correlations in viscous liquids *Phys. Rev.* E **83** 051505
[43] Shintani H and Tanaka H 2006 Frustration on the way to crystallization in glass *Nat. Phys.* **2** 200
[44] Molinero V, Sastry S and Angell C A 2006 Tuning of tetrahedrality in a silicon potential yields a series of monatomic (metal-like) glass formers of very high fragility *Phys. Rev. Lett.* **97** 075701
[45] Parmar A D and Sastry S 2015 Kinetic and thermodynamic fragilities of square well fluids with tunable barriers to bond breaking *J. Phys. Chem.* B **119** 11243
[46] Kim K, Miyazaki K and Saito S 2011 Slow dynamics, dynamic heterogeneities, and fragility of supercooled liquids confined in random media *J. Phys.: Condens. Matter* **23** 234123
[47] Chakrabarty S, Karmakar S and Dasgupta C 2015 Dynamics of glass forming liquids with randomly pinned particles *Sci. Rep.* **5** 12577
[48] Sausset F, Tarjus G and Viot P 2008 Tuning the fragility of a glass-forming liquid by curving space *Phys. Rev. Lett.* **101** 155701
[49] Alba-Simionesco C, Kivelson D and Tarjus G 2002 Temperature, density, and pressure dependence of relaxation times in supercooled liquids *J. Chem. Phys.* **116** 5033
[50] Casalini R and Roland C 2004 Thermodynamical scaling of the glass transition dynamics *Phys. Rev.* E **69** 062501
[51] Alba-Simionesco C and Tarjus G 2006 Temperature versus density effects in glassforming liquids and polymers: a scaling hypothesis and its consequences *J. Non-Cryst. Solids* **352** 4888
[52] Pedersen U R, Bailey N P, Schrøder T B and Dyre J C 2008 Strong pressure-energy correlations in van der Waals liquids *Phys. Rev. Lett.* **100** 015701
[53] Schrøder T B, Bailey N P, Pedersen U R, Gnan N and Dyre J C 2009 Pressure-energy correlations in liquids. III. Statistical mechanics and thermodynamics of liquids with hidden scale invariance *J. Chem. Phys.* **131** 234503
[54] Gnan N, Schrøder T B, Pedersen U R, Bailey N P and Dyre J C 2009 Pressure-energy correlations in liquids. IV.'Isomorphs' in liquid phase diagrams *J. Chem. Phys.* **131** 234504
[55] Schrøder T B, Gnan N, Pedersen U R, Bailey N P and Dyre J C 2011 Pressure-energy correlations in liquids. V. Isomorphs in generalized Lennard-Jones systems *J. Chem. Phys.* **134** 164505
[56] Ediger M D 2000 Spatially heterogeneous dynamics in supercooled liquids *Annu. Rev. Phys. Chem.* **51** 99
[57] Berthier L, Biroli G, Coslovich D, Kob W and Toninelli C 2012 Finite-size effects in the dynamics of glass-forming liquids *Phys. Rev.* E **86** 031502
[58] Kim K and Saito S 2013 Multiple length and time scales of dynamic heterogeneities in model glass-forming liquids: A systematic analysis of multi-point and multi-time correlations *J. Chem. Phys.* **138** 12A506
[59] Kawasaki T, Kim K and Onuki A 2014 Dynamics in a tetrahedral network glassformer: vibrations, network rearrangements, and diffusion *J. Chem. Phys.* **140** 184502
[60] Staley H, Flenner E and Szamel G 2015 Reduced strength and extent of dynamic heterogeneity in a strong glass former as compared to fragile glass formers *J. Chem. Phys.* **143** 244501

J. Stat. Mech. (2016) 074002

[61] Zaccarelli E, Sciortino F and Tartaglia P 2007 A spherical model with directional interactions. I. Static properties *J. Chem. Phys.* **127** 174501
[62] Mayer C, Sciortino F, Tartaglia P and Zaccarelli E 2010 A spherical model with directional interactions: II. Dynamics and landscape properties *J. Phys.: Condens. Matter* **22** 104110
[63] Hiwatari Y, Matsuda H, Ogawa T, Ogita N and Ueda A 1974 Molecular dynamics studies on the soft-core model *Prog. Theor. Phys.* **52** 1105
[64] Keskar N R and Chelikowsky J R 1992 Structural properties of nine silica polymorphs *Phys. Rev.* B **46** 1
[65] Elliott S 1991 Origin of the first sharp diffraction peak in the structure factor of covalent glasses *Phys. Rev. Lett.* **67** 711
[66] Nakamura T, Hiraoka Y, Hirata A, Escolar G E, Matsue K and Nishiura Y 2015 Description of medium-range order in amorphous structures by persistent homology (arXiv:1501.03611)
[67] Kob W and Andersen H C 1995 Testing mode-coupling theory for a supercooled binary Lennard-Jones mixture. II. Intermediate scattering function and dynamic susceptibility *Phys. Rev.* E **52** 4134
[68] Kob W, Roldan-Vargas S and Berthier L 2012 Spatial correlations in glass-forming liquids across the mode-coupling crossover *Phys. Procedia* **34** 70
[69] Malins A, Eggers J, Royall C P, Williams S R and Tanaka H 2013 Identification of long-lived clusters and their link to slow dynamics in a model glass former *J. Chem. Phys.* **138** 12A535
[70] Barrat J L, Badro J and Gillet P 1997 A strong to fragile transition in a model of liquid silica *Mol. Simul.* **20** 17
[71] Tanaka H 2011 Roles of bond orientational ordering in glass transition and crystallization *J. Phys.: Condens. Matter* **23** 284115
[72] Mikkelsen J Jr 1984 Self-diffusivity of network oxygen in vitreous SiO_2 *Appl. Phys. Lett.* **45** 1187
[73] Horbach J and Kob W 1999 Static and dynamic properties of a viscous silica melt *Phys. Rev.* B **60** 3169
[74] Saksaengwijit A and Heuer A 2006 Origin of the decoupling of oxygen and silicon dynamics in liquid silica as expressed by its potential energy landscape *Phys. Rev.* E **74** 051502
[75] Kawasaki T and Onuki A 2013 Slow relaxations and stringlike jump motions in fragile glass-forming liquids: breakdown of the Stokes–Einstein relation *Phys. Rev.* E **87** 012312
[76] Coslovich D and Roland C 2011 Heterogeneous slow dynamics and the interaction potential of glass-forming liquids *J. Non-Cryst. Solids* **357** 397
[77] Flenner E, Staley H and Szamel G 2014 Universal features of dynamic heterogeneity in supercooled liquids *Phys. Rev. Lett.* **112** 097801
[78] Sengupta S, Karmakar S, Dasgupta C and Sastry S 2013 Breakdown of the Stokes–Einstein relation in two, three, and four dimensions *J. Chem. Phys.* **138** 12A548
[79] Shi Z, Debenedetti P G and Stillinger F H 2013 Relaxation processes in liquids: variations on a theme by Stokes and Einstein *J. Chem. Phys.* **138** 12A526
[80] Xia X and Wolynes P G 2001 Microscopic theory of heterogeneity and nonexponential relaxations in supercooled liquids *Phys. Rev. Lett.* **86** 5526
[81] Dyre J C 2007 Ten themes of viscous liquid dynamics *J. Phys.: Condens. Matter* **19** 205105
[82] Heuer A 2008 Exploring the potential energy landscape of glass-forming systems: from inherent structures via metabasins to macroscopic transport *J. Phys.: Condens. Matter* **20** 373101
[83] Saika-Voivod I, Poole P H and Sciortino F 2001 Fragile-to-strong transition and polyamorphism in the energy landscape of liquid silica *Nature* **412** 514
[84] Saika-Voivod I, Sciortino F and Poole P H 2004 Free energy and configurational entropy of liquid silica: fragile-to-strong crossover and polyamorphism *Phys. Rev.* E **69** 041503
[85] Speck T, Royall C P and Williams S R 2014 Liquid–liquid phase transition in an atomistic model glass former (arXiv:1409.0751)
[86] Saika-Voivod I, Sciortino F, Grande T and Poole P H 2004 Phase diagram of silica from computer simulation *Phys. Rev.* E **70** 061507
[87] Berthier L and Tarjus G 2011 The role of attractive forces in viscous liquids *J. Chem. Phys.* **134** 214503
[88] Scopigno T, Ruocco G, Sette F and Monaco G 2003 Is the fragility of a liquid embedded in the properties of its glass? *Science* **302** 849
[89] Mauro N, Blodgett M, Johnson M, Vogt A and Kelton K 2014 A structural signature of liquid fragility *Nat. Commun.* **5** 4616
[90] Qiu X and Ediger M 2003 Length scale of dynamic heterogeneity in supercooled D-sorbitol: comparison to model predictions *J. Phys. Chem.* B **107** 459
[91] Berthier L, Biroli G, Bouchaud J P, Cipelletti L, El Masri D, L'Hôte D, Ladieu F and Pierno M 2005 Direct experimental evidence of a growing length scale accompanying the glass transition *Science* **310** 1797

J. Stat. Mech. (2016) 074002